

AD-A069 107

ARMY ARMAMENT RESEARCH AND DEVELOPMENT COMMAND ABERD--ETC F/G 19/4
THE EPSILON-PHASE HUGONIOT OF ROLLED HOMOGENEOUS ARMOR.(U)

MAR 79 G HAUVER, A MELANI

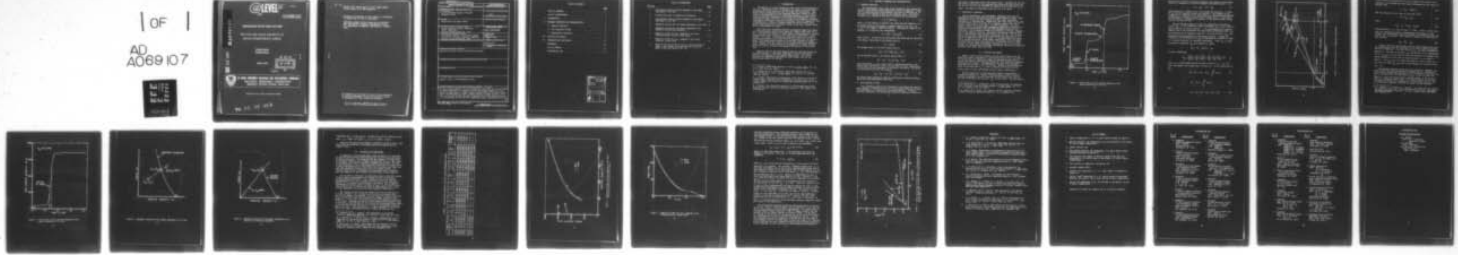
UNCLASSIFIED

ARBRL-MR-02909

SBIE-AD-E430 226

NL

| OF |
AD
A069107



END
DATE
FILMED

7-79
DDC

AD A069107

DDC FILE COPY



US ARMY ARMAMENT RESEARCH AND DEVELOPMENT COMMAND
BALLISTIC RESEARCH LABORATORY
ABERDEEN PROVING GROUND, MARYLAND

Approved for public release; distribution unlimited.

79 05 07 024

(12) **LEVEL** III

AD-E430 226

MEMORANDUM REPORT ARBRL-MR-02909

THE EPSILON-PHASE HUGONIOT OF
ROLLED HOMOGENEOUS ARMOR

George Hauver
Angelo Melani

March 1979



Destroy this report when it is no longer needed.
Do not return it to the originator.

Secondary distribution of this report by originating
or sponsoring activity is prohibited.

Additional copies of this report may be obtained
from the National Technical Information Service,
U.S. Department of Commerce, Springfield, Virginia
22161.

The findings in this report are not to be construed as
an official Department of the Army position, unless
so designated by other authorized documents.

*The use of trade names or manufacturers' names in this report
does not constitute endorsement of any commercial product.*

UNCLASSIFIED

SECURITY CLASSIFICATION OF THIS PAGE (When Data Entered)

REPORT DOCUMENTATION PAGE		READ INSTRUCTIONS BEFORE COMPLETING FORM
1. REPORT NUMBER MEMORANDUM REPORT ARBRL-MR-02909	2. GOVT ACCESSION NO.	3. RECIPIENT'S CATALOG NUMBER
4. TITLE (and Subtitle) The Epsilon-Phase Hugoniot of Rolled Homogeneous Armor	5. TYPE OF REPORT & PERIOD COVERED Final	
7. AUTHOR(s) George Hauver and Angelo Melani	6. PERFORMING ORG. REPORT NUMBER	
9. PERFORMING ORGANIZATION NAME AND ADDRESS US Army Ballistic Research Laboratory (ATTN: DRDAR-BLT) Aberdeen Proving Ground, MD 21005	10. PROGRAM ELEMENT, PROJECT, TASK AREA & WORK UNIT NUMBERS RDTGE 1L662618AH80	
11. CONTROLLING OFFICE NAME AND ADDRESS USA Armament Research & Development Command USA Ballistic Research Laboratory (DRDAR-BL) Aberdeen Proving Ground, MD 21005	12. REPORT DATE MARCH 1979	
14. MONITORING AGENCY NAME & ADDRESS (if different from Controlling Office)	13. NUMBER OF PAGES 27	
	15. SECURITY CLASS. (of this report) Unclassified	
	15a. DECLASSIFICATION/DOWNGRADING SCHEDULE	
16. DISTRIBUTION STATEMENT (of this Report) Approved for public release; distribution unlimited.		
17. DISTRIBUTION STATEMENT (of the abstract entered in Block 20, if different from Report)		
18. SUPPLEMENTARY NOTES		
19. KEY WORDS (Continue on reverse side if necessary and identify by block number) Hugoniot; armor; rolled homogeneous armor		
20. ABSTRACT (Continue on reverse side if necessary and identify by block number) bet 2972 The epsilon-phase Hugoniot of rolled homogeneous armor (RHA) has been determined by impact experiments and compared with the epsilon-phase Hugoniot of iron. Results for RHA suggest a slightly greater volume offset at the alpha-epsilon phase transformation and slightly stiffer behavior at higher stresses. Rise-time of the second plastic wave and attenuation of the first plastic wave are in close agreement for RHA and iron, suggesting similar transformation kinetics.		

TABLE OF CONTENTS

	<u>Page</u>
TABLE OF CONTENTS.	3
LIST OF ILLUSTRATIONS.	5
I. INTRODUCTION	7
II. MEASURED PARAMETERS AND EXPERIMENTATION.	8
A. Hugoniot Equations	8
B. Test Specimens of RHA.	8
C. Experimental Techniques.	9
III. ANALYSIS AND RESULTS	9
IV. DISCUSSION AND CONCLUSIONS	17
REFERENCES	23
LIST OF SYMBOLS.	24
DISTRIBUTION LIST.	25

ACCESSION for	
NTIS	White Section <input checked="" type="checkbox"/>
DDC	Buff Section <input type="checkbox"/>
UNANNOUNCED	<input type="checkbox"/>
JUSTIFICATION	_____
BY	
DISTRIBUTION/AVAILABILITY CODES	
Dist.	STATE <input type="checkbox"/> DOD <input type="checkbox"/> SPECIAL <input type="checkbox"/>
A	

LIST OF ILLUSTRATIONS

<u>FIG. NO.</u>		<u>Page</u>
1	Free-surface velocity profile measured in the impact experiment at 23.6 GPa.	10
2	Distance-Time plot in laboratory coordinates.	12
3	Free-surface velocity profile measured in the impact experiment at 34.5 GPa.	14
4	Impedance solution for the impact experiment at 34.5 GPa.	15
5	Impedance solution for the impact experiments with explosively accelerated impactors	16
6	Hugoniots of RHA and iron, compared in the shock velocity-particle velocity ($U-u$) plane.	19
7	Hugoniots of RHA and iron, compared in the stress-(relative) volume plane	20
8	Stress at the top of the P1 wave vs. driving stress at impact. The straight lines are data fits using the model of Horie and Duvall (Ref. 10)	22

I. THE INTRODUCTION

The Hugoniot of rolled homogeneous armor (RHA) has been measured as part of a coordinated effort to determine the dynamic and quasi-static properties of steels which are used for armors and penetrators. This study of RHA has benefited from preceding shock-wave studies of iron. Barker's reinterpretation of the alpha-phase Hugoniot of iron¹ and his collaboration with Hollenbach in the shock-wave investigation of the alpha-epsilon phase transition in iron² have been invaluable, providing experimental techniques, analytical procedures, data for comparisons, and interpretations. Further information about the shock-induced alpha-epsilon phase transition in iron has recently come from a careful experimental investigation by Forbes.³

RHA, like iron, transforms from the low-pressure alpha (bcc) phase to the high-pressure epsilon (hcp) phase at a shock stress close to 13 GPa. Just below the transition stress impact loading produces a two-wave stress profile which consists of an elastic wave followed by a slower Plastic 1 (P1) wave. Just above the transition stress the P1 wave is followed by a Plastic 2 (P2) wave which is associated with the epsilon phase. The stress profile reverts to a two-wave structure at higher shock stresses where the velocity of the P2 wave exceeds the maximum P1 value. Finally, a single shock wave is propagated at higher stresses where the velocity of the P2 wave exceeds the velocity of the elastic wave.

Hugoniot data for the alpha phase of RHA were obtained earlier and have been reported.⁴ Additional experiments have been performed to establish the Hugoniot for the epsilon phase of RHA. This report describes the experiments and analysis, and presents data for the epsilon phase from 13 to 135 GPa.

¹L. M. Barker, "Alpha-Phase Hugoniot of Iron", J. Appl. Phys., Vol. 46, No. 6, June 1975, pp. 2544-7.

²L. M. Barker and R. E. Hollenbach, "Shock-Wave study of the $\alpha \rightleftharpoons \epsilon$ Phase Transition in Iron", J. Appl. Phys., Vol. 45, No. 11, November 1974, pp. 4872-87.

³J. W. Forbes, "Experimental Investigation of the Kinetics of the Shock-Induced Alpha to Epsilon Phase Transformation in Armco Iron", Naval Surface Weapons Center/White Oak Laboratory Technical Report No. 77-137, December 1977.

⁴G. E. Hauer, "The Alpha-Phase Hugoniot of Rolled Homogeneous Armor", Ballistic Research Laboratory Memorandum Report No. 2651, August 1976, AD #B012871L.

II. MEASURED PARAMETERS AND EXPERIMENTATION

A. Hugoniot Equations

The thermodynamic states that can be reached by shock compression define a curve in the stress-volume plane called the Hugoniot. In the case of a multiple-wave stress profile, the stress on the Hugoniot is the sum of the stresses carried by the different waves. The stress increase, $\sigma - \sigma_i$, carried by each wave is given by the relationship,

$$\sigma - \sigma_i = \rho_i U(u - u_i), \quad (1)$$

where ρ_i is the density of material into which the wave advances, U is the shock velocity with respect to material ahead of the wave, and $(u - u_i)$ is the change in particle velocity. The specific volume on the Hugoniot, V , is given by the relationship,

$$V = V_i [1 - (u - u_i)/U], \quad (2)$$

where $V_i = 1/\rho_i$. In the case of iron or RHA, the stress may be carried by three waves. The stress in the elastic wave is

$$\sigma_e = \rho_o U e u_e, \quad (3)$$

the maximum stress in the first plastic wave is

$$\sigma_{p1} = \sigma_e + \rho_e U_{p1} (u_{p1} - u_e), \quad (4)$$

and the maximum stress in the second plastic wave is

$$\sigma_{p2} = \sigma_{p1} + \rho_{p1} U_{p2} (u_{p2} - u_{p1}), \quad (5)$$

where subscripts o, e, p1, and p2 refer to unstressed material, the elastic wave, the Plastic 1 wave, and the Plastic 2 wave, respectively. If the wave velocity is measured in laboratory coordinates, the expression for stress in the P2 wave becomes,

$$\sigma_{p2} = \sigma_{p1} + \rho_{p1} (U_{p2}^* - u_{p1}) (u_{p2} - u_{p1}) \quad (6)$$

The epsilon-phase Hugoniot of RHA was established by measuring impact, shock wave, and free-surface velocities.

B. Test Specimens of RHA

Test specimens prepared for measurements to determine the epsilon-phase Hugoniot of RHA were similar to test specimens previously prepared for measurements to determine the alpha-phase Hugoniot. Chemical analyses, hardnesses, and preparation procedures reported in Reference 4

also apply to specimens used in the current tests. Specimens for all but one of the current tests were prepared from 13-mm thick plate stock; for the test at 16.0 GPa, the specimen was prepared from 100-mm thick plate stock. The density of RHA plate stock was 7.84×10^3 kg/m³.

C. Experimental Techniques

Both interferometric and photographic techniques were used for measurements which established the epsilon-phase Hugoniot of RHA. Peak stresses up to 34.5 GPa were obtained by plane impact experiments performed in a light-gas gun. Symmetrical, RHA → RHA, impacts were used at peak stresses up to 23.6 GPa, but a tungsten impactor was used to achieve a peak stress of 34.5 GPa. In these experiments, the free-surface velocity of impacted RHA specimens was measured continuously by VISAR-type instrumentation (Velocity Interferometer System for Any Reflector)⁵, and a sequence of electrical contactors provided a measurement of the impactor velocity. Explosively accelerated impactors were used to obtain higher peak stresses of 63.6 and 135 GPa. The two-wave region was bypassed in going from a three-wave shock structure at 34.5 GPa to a single shock wave at 63.6 GPa. In the experiments with explosively accelerated plates, streak camera measurements utilized changes in reflectance to detect the arrival of a strong shock wave at a free surface⁶. Streak camera measurements provided the shock wave velocity through RHA specimens and the average free-surface velocity of a Type 304 stainless steel plate which held them.

III. ANALYSIS AND RESULTS

Figure 1 shows the free-surface velocity profile measured in the symmetrical impact experiment at a peak stress of 23.6 GPa. The elastic, P₁, and P₂ waves are identified along with perturbations believed to result from elastic reverberations between the free surface and approaching plastic wave fronts. The midpoint of each wave front was used to establish wave arrival at the free surface. Midpoints are indicated by small circles, and times t₁, t₂, and t₄ identify the arrivals of the elastic wave, P₁ wave, and residue of the P₂ wave, respectively.

Analysis applicable to the alpha-phase Hugoniot measurements is included in Reference 4. Briefly, the free-surface velocity profile, specimen dimensions, and prior knowledge of the elastic-wave velocity are used to determine the velocity, U_{p1}, of the P₁ wave. For the elastic

⁵L. M. Barker and R. E. Hollenbach, "Laser Interferometer for Measuring High Velocities of any Reflecting Surface", *J. Appl. Phys.*, Vol. 43, No. 11, November 1972, pp. 4669-75.

⁶G. E. Hauver and A. Melani, "The Hugoniot of 5083 Aluminum", Ballistic Research Laboratory Memorandum Report No. 2345, December 1973.

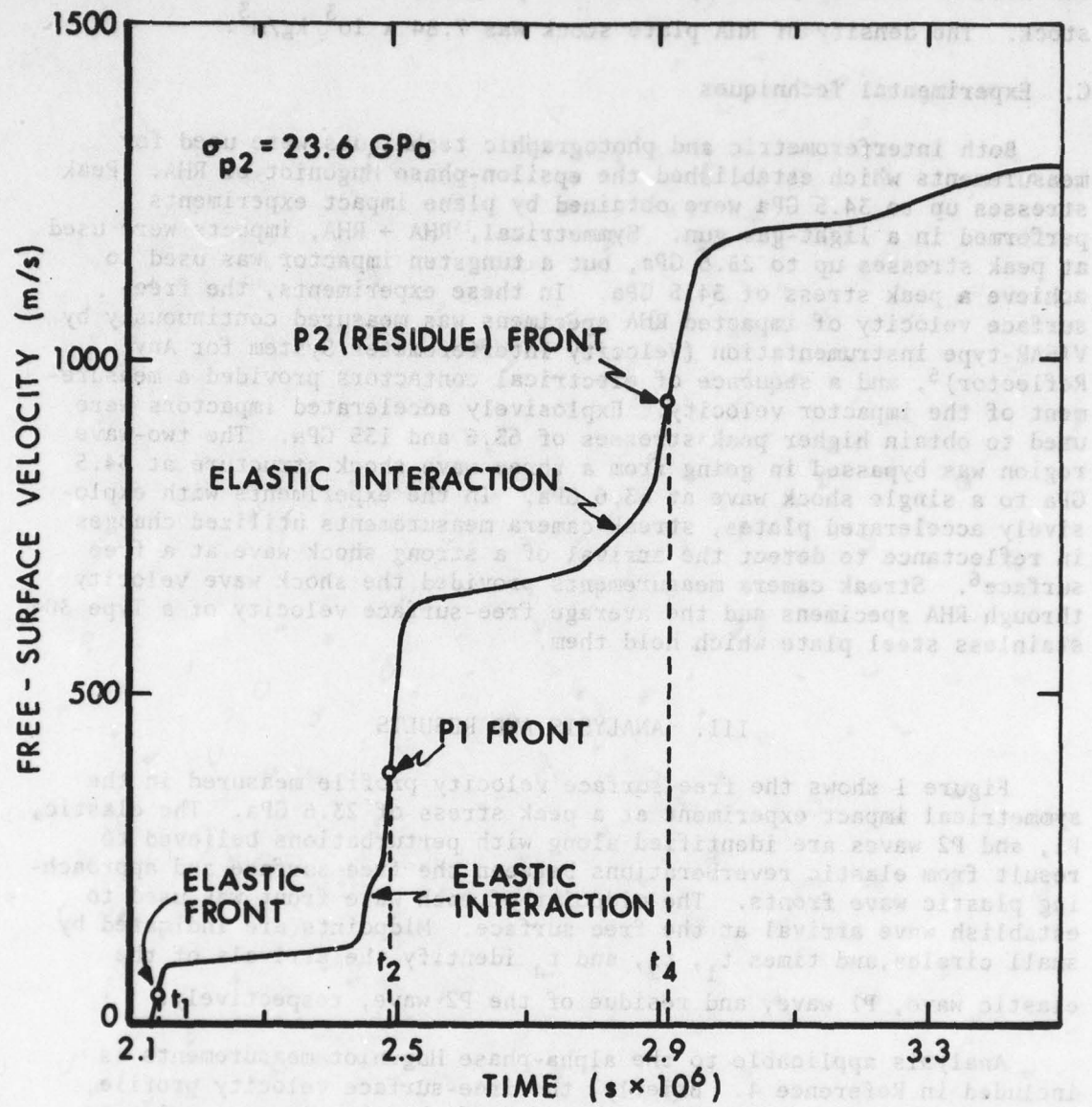


Figure 1. Free-surface velocity profile measured in the impact experiment at 23.6 GPa.

wave and the P1 wave at the phase transition, the change in free-surface velocity is assumed to be twice the change in particle velocity, i.e.,

$$(u_f - u_{fi}) = 2(u - u_i), \quad (7)$$

where subscript, f, refers to the free surface and subscript, i, refers to the initial condition (before wave arrival). The adequacy of this assumption was supported by the investigation of alpha-phase RHA reported in Reference 4. Forbes³ cites the work of Walsh, et.al.⁵, and Barker and Hollenbach² in defending the adequacy of the "factor-of-two" assumption for the case of iron.

The epsilon-phase Hugoniot of RHA was established by evaluating u_{p2} and U_{p2} . In the symmetrical impact experiments, $u_{p2} = u_o/2$, where u_o is the velocity of the RHA impactor. In the experiment with a tungsten impactor and in the experiments with explosively accelerated plates, u_{p2} was determined by an impedance solution⁵. The shock velocity, U_{p2} , was determined from measurements of free-surface velocity. Assumptions involved in the determination of U_{p2} are explained by reference to Figure 2, a distance-time plot in laboratory coordinates. Point (x_3, t_3) must be located to establish U_{p2}^* (See Equation 6), where

$$U_{p2}^* = (x_3 - x_0)/(t_3 - t_0)$$

It can be shown that,

$$U_{p2}^* = \frac{U_2(x_2 - x_0) + U_1(x_4 - x_0) - U_1 U_2(t_4 - t_2)}{U_2(t_4 - t_0) + U_1(t_2 - t_0) - (x_4 - x_2)} \quad (8)$$

Time, t_0 , is established from the specimen thickness, $(x_1 - x_0)$, and prior knowledge of the elastic-wave velocity, U_e . In the expression for U_{p2}^* ,

$$(x_2 - x_0) = (x_1 - x_0) + \int_{t_1}^{t_2} u_f dt, \quad (9)$$

$$(x_4 - x_2) = \int_{t_2}^{t_4} u_f dt, \quad (10)$$

and,

$$(x_4 - x_0) = (x_2 - x_0) + (x_4 - x_2). \quad (11)$$

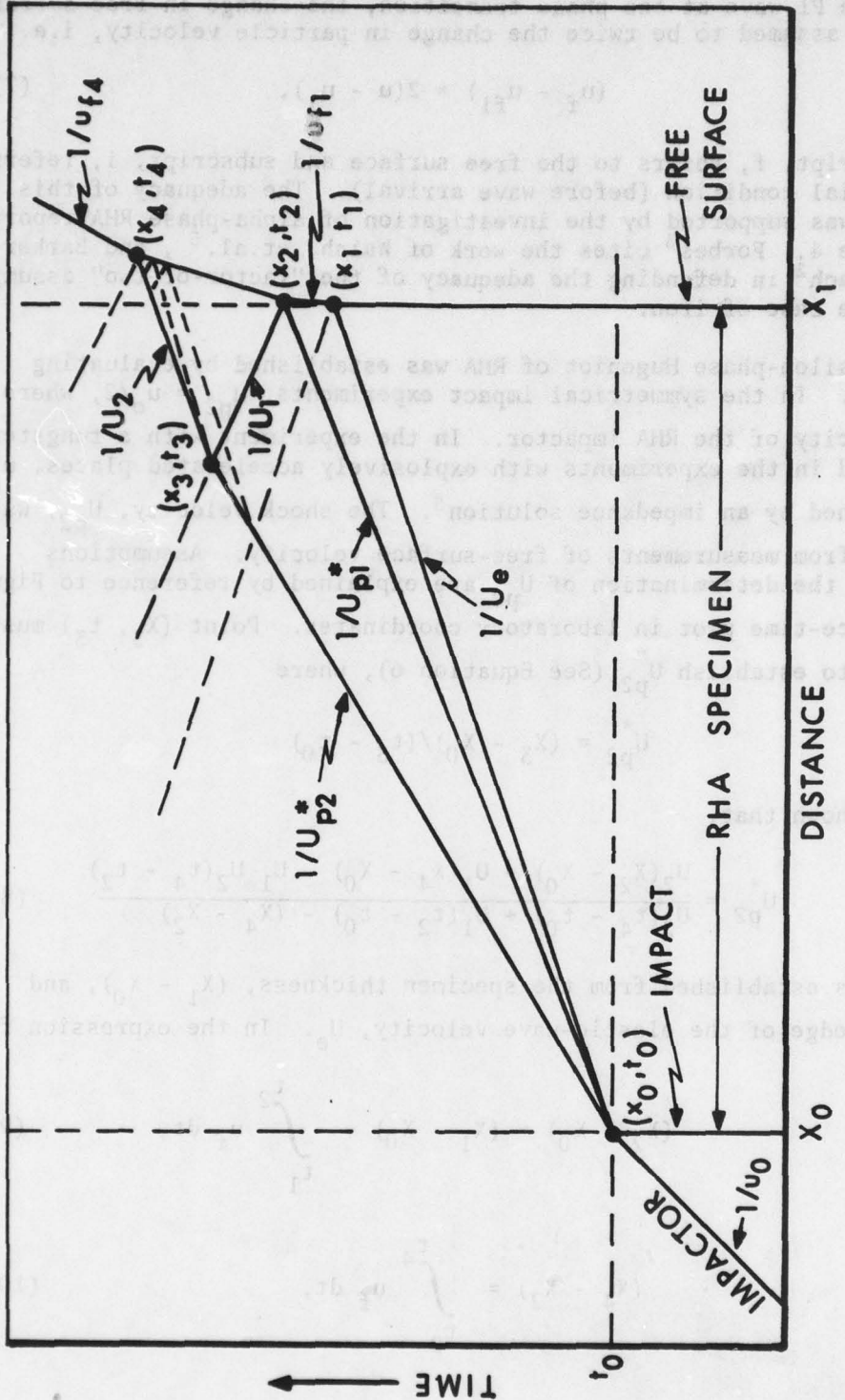


Figure 2. Distance-Time plot in laboratory coordinates.

Unlike Forbes³ who assumed that U_1 and U_2 depend on the elastic-wave velocity, it is assumed here that elastic reverberations can usually be ignored, with

$$U_1 \approx U_{p1} - (u_{f2}/2). \quad (12)$$

When the residue of the P2 wave is less than 13 GPa,

$$U_2 \approx U_{p1} + u_{f2}, \quad (13)$$

where,

$$U_{p1} = C_o + S (u_{f4} - u_{f2})/2. \quad (14)$$

(From Reference 4, $C_o = 4510$ m/s and $S = 1.430$). Figure 1 offers some basis for ignoring the elastic reverberations which appear in each instance as a perturbation below the midpoint of the wavefront where the arrival time is evaluated. With respect to material into which the P2 wave advances,

$$U_{p2} = U_{p2}^* - u_{p1}. \quad (15)$$

Figure 3 shows the free-surface velocity profile obtained by velocity interferometry from the experiment at 34.5 GPa in which a tungsten impactor was employed. The shock velocity, U_{p2} , was again determined by Equation 8. The particle velocity, u_{p2} , was located at the intersection of the $(\rho_{p1} U_{p2})$ line for RHA with the known Hugoniot for tungsten⁷ which passes through zero stress and the impact velocity, u_o , as shown in Figure 4. The $(\rho_{p1} U_{p2})$ line comes from Equation 5 and in this case is the line with slope $(\rho_{p1} U_{p2})$ which passes through the transition state (u_{p1}, σ_{p1}) .

Epsilon-phase Hugoniot points were also obtained by impedance solutions in the tests with explosively accelerated plates. The measured shock velocity through RHA specimens on the 304 stainless steel plate was used to establish the line with slope $(\rho_o U_{p2})$ in the σ - u plane (See Figure 5). This line intersected the release adiabat of 304 stainless steel at the Hugoniot state in RHA. The release adiabat of the stainless steel was located by a measurement of free-surface velocity, and was generated by assuming a constant $\gamma\rho$, where γ is the Gruneisen

⁷R. G. McQueen, S. P. Marsh, W. J. Carter, J. N. Fritz, and J. W. Taylor, "The Equation of State of Solids from Shock Wave Studies", High Velocity Impact Phenomena, edited by R. Kinslow, Academic Press, New York, 1970, Chapter VII.

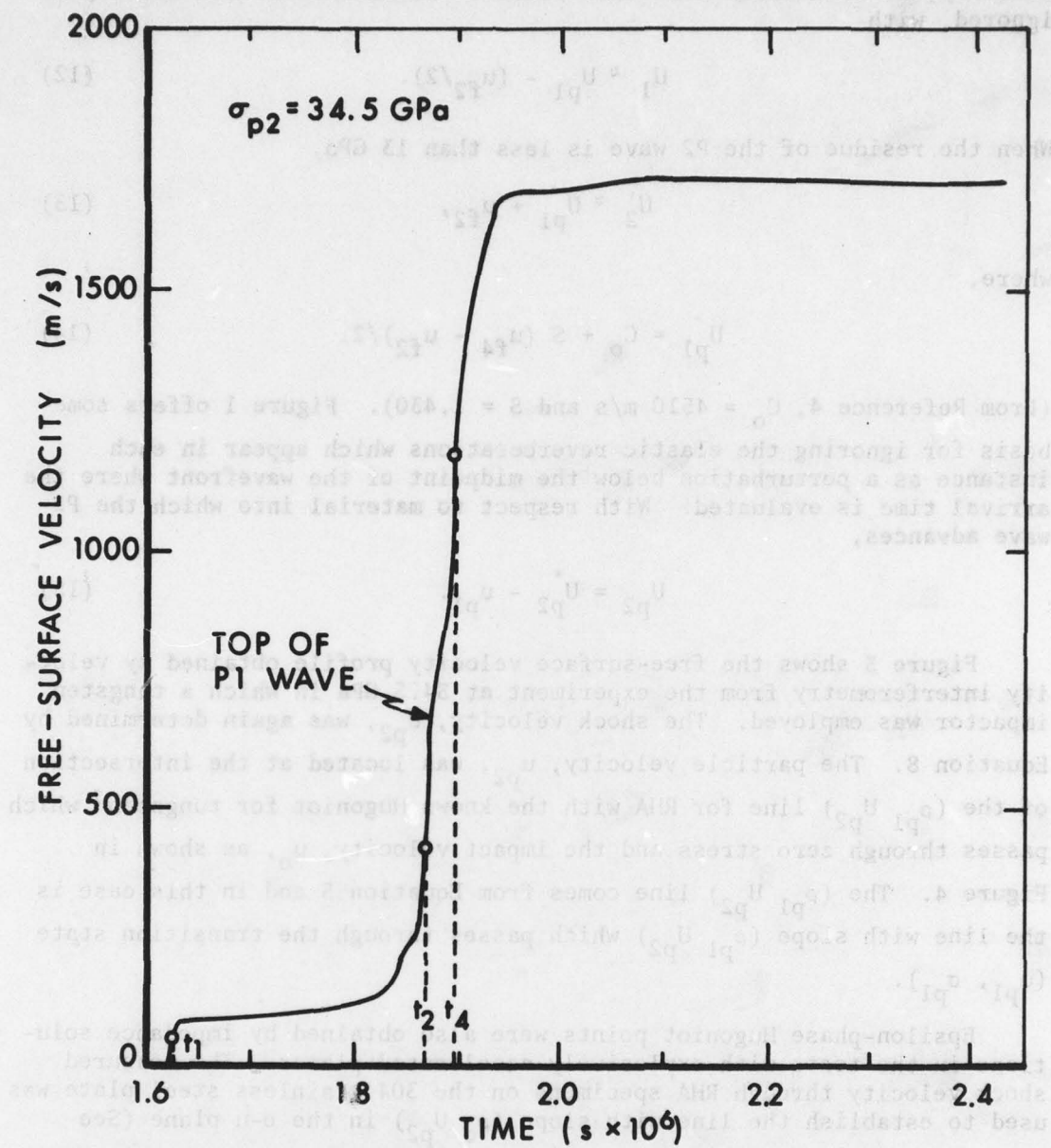


Figure 3. Free-surface velocity profile measured in the impact experiment at 34.5 GPa.

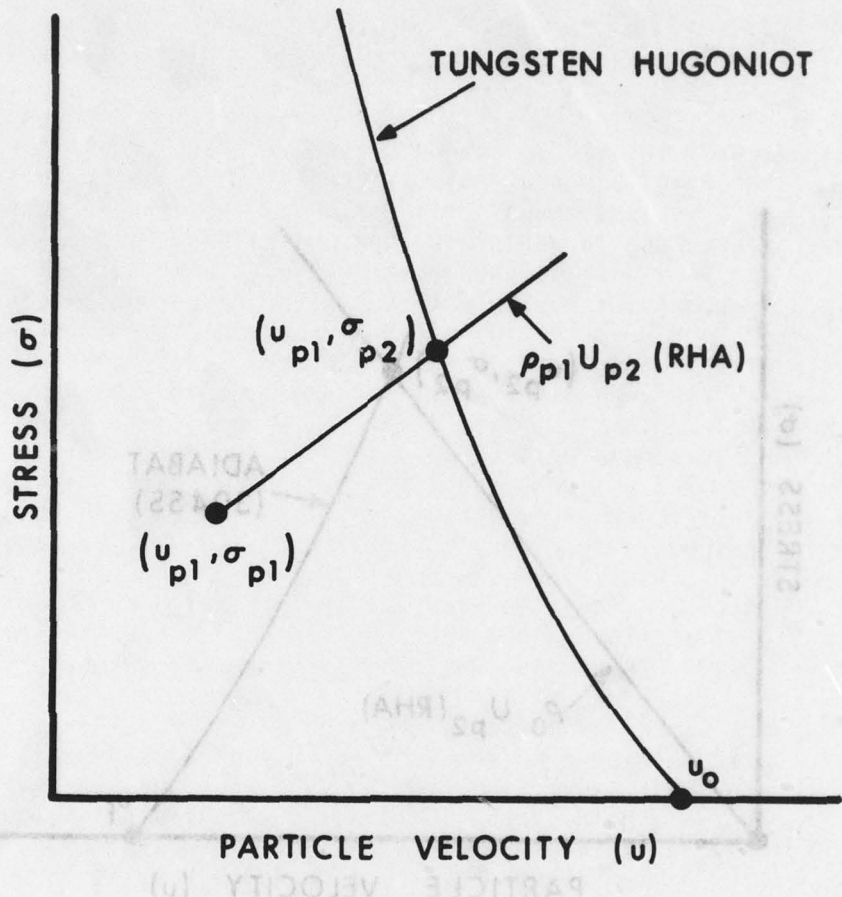


Figure 4. Impedance solution for the impact experiment at 34.5 GPa.

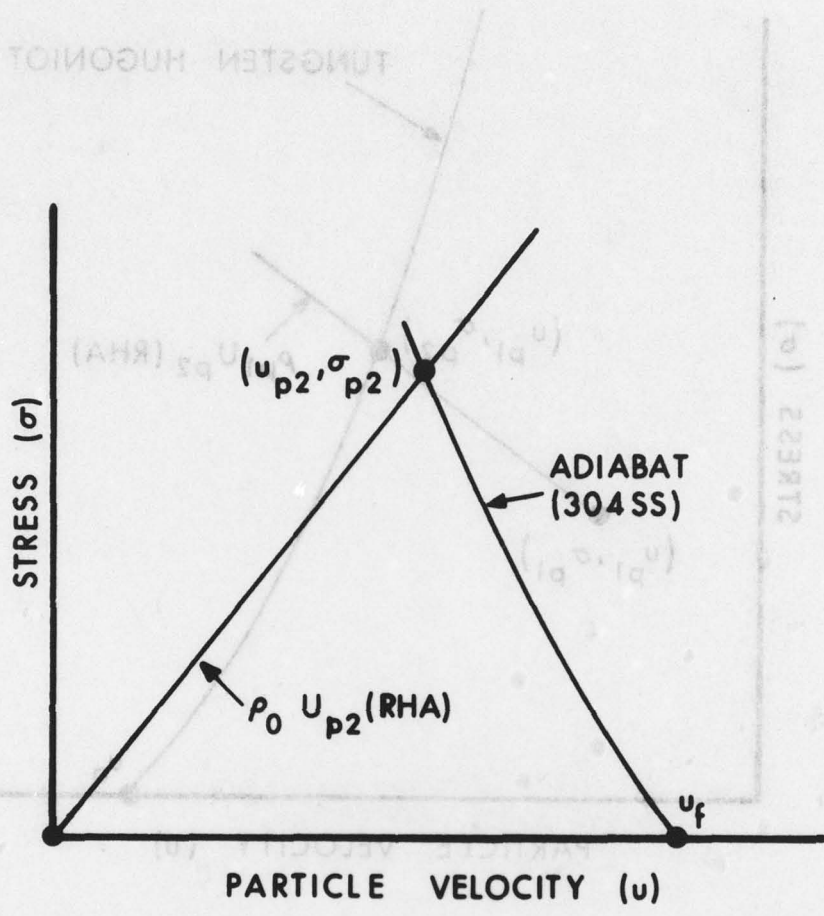


Figure 5. Impedance solution for the impact experiments with explosively accelerated impactors.

coefficient and ρ is the density. The data used for 304 stainless steel⁷ were: $\rho_0 = 7.896 \times 10^3 \text{ kg/m}^3$; $\gamma_0 = 2.17$; $U = 4569 + 1.490 u$.

Data for the epsilon-phase Hugoniot of RHA are listed in Table 1 and are plotted as extensions of preceding alpha-phase Hugoniot data in Figures 6 and 7.

IV. DISCUSSION AND CONCLUSIONS

The Hugoniot of epsilon-phase RHA, shown in Figure 7, is displaced to the left of the epsilon-phase Hugoniot of iron at stresses just above the phase transition. This suggests that RHA undergoes a volume offset at the phase transition which slightly exceeds that of iron. This result is consistent with results reported by Takahashi and Bassett⁸ who used X-ray diffraction at static high pressures to show that the volume offset at phase transformations in iron-nickel alloys increases with nickel content (RHA specimens contained from 3.0 to 3.5 percent nickel). At stresses above 50 GPa, the Hugoniot of epsilon-phase RHA is displaced above the Hugoniot of epsilon-phase iron indicating stiffer behavior.

For at least 5.0 GPa above the transition stress in RHA the risetime of the P2 wave is approximately $0.3\mu\text{s}$ based on the 5 to 95 percent criterion adopted by Forbes³. This risetime is consistent with the corresponding 0.2 to $0.3\mu\text{s}$ risetime of the P2 wave in iron reported by Novikov, et. al.⁹, Barker and Hollenbach², and Forbes, and it suggests transformation kinetics similar to those of iron. At 23.6 GPa the risetime of the P2 wave in RHA has decreased to approximately $0.1\mu\text{s}$, again in close agreement with results for iron reported in Reference 2.

The risetime of the P2 wave was found to be $0.07\mu\text{s}$ in the test at 34.5 GPa. However, this risetime may not be accurate because the P1 and P2 waves appear to be merging. As they merge, the feature identified as the top of the P1 wave may be displaced to higher velocities (See Figure 3). In this test, the transition stress has apparently increased to 13.74 GPa. Although the data for iron by Barker and Hollenbach reveal an increase in the amplitude of the P1 wave with increasing driving stress, it can be shown that an increase to 13.74 GPa is unreasonably large for RHA in this test. Horie and Duvall¹⁰, in their treatment of wave propagation in a phase transforming material, assume the material to be

⁸T. Takahashi and W. A. Bassett, "The Composition of the Earth's Interior", Scientific American, Vol. 212, No. 6, June 1965, pp. 100-8.

⁹S. A. Novikov, I. I. Divnov, and A. G. Ivanov, "Investigation of the Structure of Compressive Shock Waves in Iron and Steel", Sov. Phys. - JTEP, Vol. 20, No. 3, March 1965, pp. 545-6.

¹⁰Y. Horie and G. E. Duvall, "Shock Waves and the Kinetics of Solid-Solid Transitions", Proceedings of the U.S. Army Symposium on Solid Mechanics, Watertown, Mass., AMMRC MS 68-09, September 1968.

TABLE 1. Epsilon-Phase Hugoniot Data for Rolled Homogeneous Armor

Test	RHA Stock mm	$(X_1 - X_0)$ mm	u_e m/s	σ_e GPa	$\frac{V_e}{V_0}$	u_{p1} m/s	U_{p1} m/s	$\frac{V_{p1}}{V_0}$	σ_{p1} GPa	u_{p2} m/s	U_{p2} m/s	$\frac{\sigma_{p2}}{\sigma_e}$	$\frac{V_{p2}}{V_0}$	Risetime of P2 Wave μs
538	100	6.327	43	1.96	0.9926	321	4995	12.93	0.9374	456	2671	16.0	0.8900	0.30
510	13	9.517	46	2.10	0.9921	322	4962	12.95	0.9368	505	2951	17.4	0.8788	0.32
529	13	12.507	45	2.06	0.9923	318	4982	12.80	0.9379	645	3994	23.6	0.8603	0.10
540	13	9.469	45.5	2.08	0.9922	339	5030	13.74	0.9343	867	4694	34.5	0.8292	0.07
"	"	"	"	"	"	(322)	(4971)	(12.95)	(0.9370)	(868)	(4708)	(34.5)	0.8284	"
553	13	4.742								1337	6064	63.6	0.7795	
554	13	4.724								2243	7651	135	0.7068	

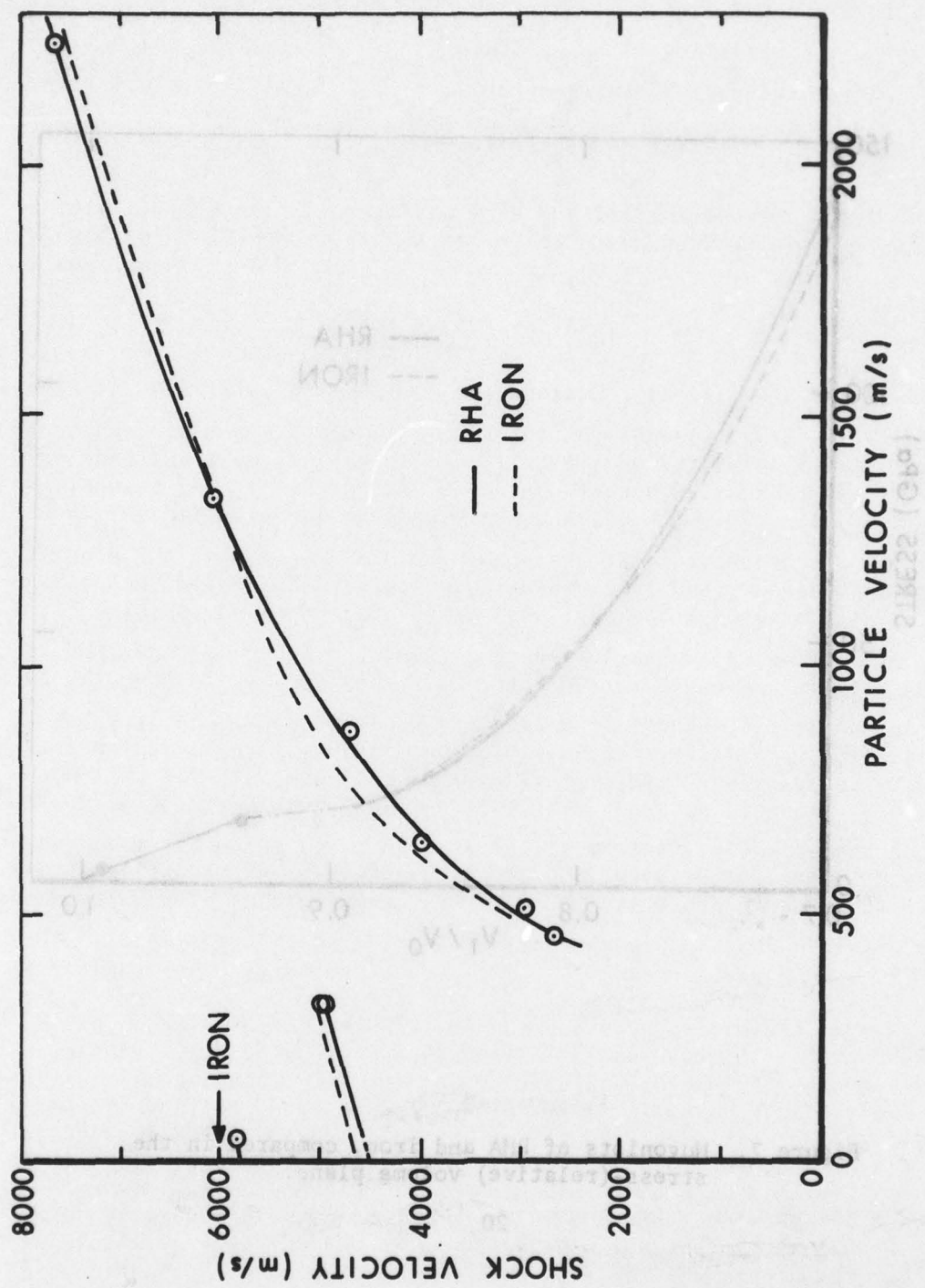


Figure 6. Hugoniots of RHA and iron, compared in the shock velocity-particle velocity ($U-u$) plane.

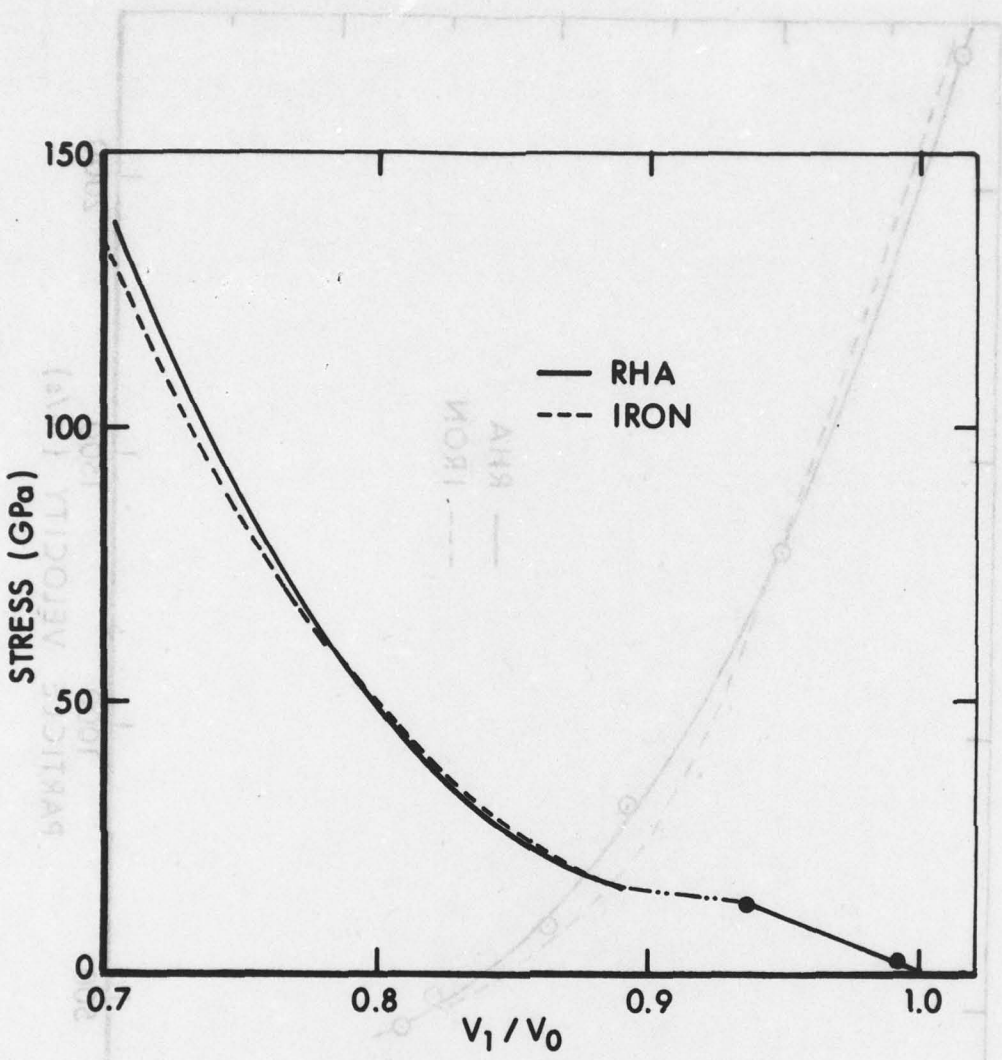


Figure 7. Hugoniots of RHA and iron, compared in the stress-(relative) volume plane.

initially overdriven along a metastable extension of the Hugoniot for the low-pressure phase. The overdriven material then relaxes into the high-pressure phase. In the Horie-Duvall model, stress in the P1 wave, σ_{p1} , changes as the wave travels away from the impacted surface, decreasing from the initial overdriven stress, σ_d , to a stress, $\sigma_{p1\infty}$, after long travel times. Stress in the P1 wave is given by the expression,

$$\sigma_{p1} = \sigma_{p1\infty} + (\sigma_d - \sigma_{p1\infty}) \exp(-t/2\tau), \quad (16)$$

where t is time after impact and τ is the relaxation time which is assumed to be constant. The time, t , is given approximately by the expression,

$$t = k (X_1 - X_0)/U_{p1}, \quad (17)$$

where $(X_1 - X_0)$ is the specimen thickness, U_{p1} is the velocity of the P1 wave, and k is a constant. The constant, k , appears because time, t , is less than the transit time of the P1 wave; the reflected elastic wave in RHA reduces the stress in the following P1 wave by approximately 2.0 GPa and no further attenuation should occur after $\sigma_{p1} \leq \sigma_{p1\infty}$ (See Reference 2).

For both RHA and iron, $k \approx 0.92$. Equation 16 represented the data of Barker and Hollenbach within approximately ± 0.1 GPa. However, a τ and $\sigma_{p1\infty}$ could not be found to produce this level of agreement with the data for RHA, and the problem seemed to be associated with the location of the datum point of Test 540 ($\sigma_{p2} = 34.5$ GPa). Since the risetime of the P2 waves in RHA is approximately the same as reported for iron, it was assumed that transformation kinetics might be similar and that the relaxation time for iron might be applicable for RHA. The results for RHA, using $\tau = 0.17\mu s$ and $\sigma_{p1\infty} = 12.80$ GPa, are shown in Figure 8. The data, except for the datum point of Test 540, are closely represented and a stress of 12.95 GPa is predicted for the P1 wave in Test 540. Data associated with this adjusted value of σ_{p1} are shown in parentheses in Table 1; the datum point for the epsilon phase undergoes negligible change as a result of this adjustment.

The epsilon-phase Hugoniot of RHA has been determined at stresses up to 135 GPa. There is close agreement with the Hugoniot of iron over the entire stress range, with only minor displacements. The volume offset at the alpha-epsilon phase transition in RHA is slightly greater, and the response of RHA at higher stresses is slightly stiffer. On the basis of risetime in the P2 wave and relaxation time in the Horie-Duvall model, the transformation kinetics in RHA and iron should be similar. Similar close agreement between the Hugoniots of RHA and iron was also found in the preceding study of the alpha phase in which the linear ($U-u$) relationships of RHA and iron were essentially parallel and displaced predictably by the difference in bulk velocities at room temperature and pressure.

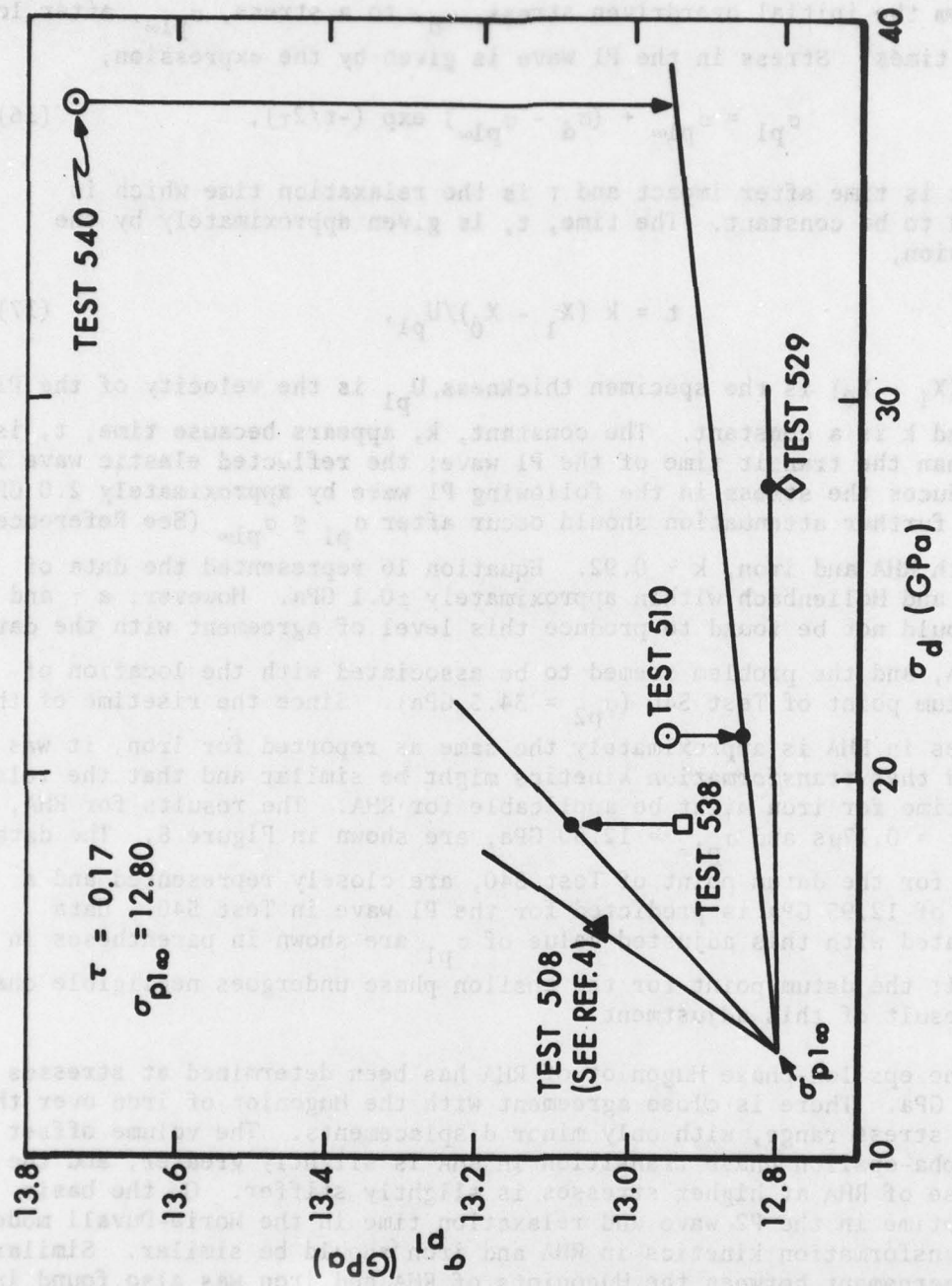


Figure 8. Stress at the top of the P1 wave vs. driving stress at impact.
The straight lines are data fits using the model of Horie and Duvall (Ref. 10).

REFERENCES

1. L. M. Barker, "Alpha-Phase Hugoniot of Iron", J. Appl. Phys., Vol. 46, No. 6, June 1975, pp. 2544-7.
2. L. M. Barker and R. E. Hollenbach, "Shock-Wave Study of the $\alpha \neq \epsilon$ Phase Transition in Iron", J. Appl. Phys., Vol. 45, No. 11, November 1974, pp. 4872-87.
3. J. W. Forbes, "Experimental Investigation of the Kinetics of the Shock-Induced Alpha to Epsilon Phase Transformation in Armco Iron", Naval Surface Weapons Center/White Oak Laboratory Technical Report No. 77-137, December 1977.
4. G. E. Hauver, "The Alpha-Phase Hugoniot of Rolled Homogeneous Armor", Ballistic Research Laboratory Memorandum Report No. 2651, August 1976. AD #B012871L.
5. L. M. Barker and R. E. Hollenbach, "Laser Interferometer for Measuring High Velocities of any Reflecting Surface", J. Appl. Phys., Vol. 43, No. 11, November 1972, pp. 4669-75.
6. G. E. Hauver and A. Melani, "The Hugoniot of 5083 Aluminum", Ballistic Research Laboratory Memorandum Report No. 2345, December 1973. (AD #773669)
7. R. G. McQueen, S. P. Marsh, W. J. Carter, J. N. Fritz, and J. W. Taylor, "The Equation of State of Solids from Shock Wave Studies", High Velocity Impact Phenomena, edited by R. Kinslow, Academic Press, New York, 1970, Chapter VII.
8. T. Takahashi and W. A. Bassett, "The Composition of the Earth's Interior", Scientific American, Vol. 212, No. 6, June 1965, pp. 100-8.
9. S. A. Novikov, I. I. Divnov, and A. G. Ivanov, "Investigation of the Structure of Compressive Shock Waves in Iron and Steel", Sov. Phys. - JETP, Vol. 20, No. 3, March 1965, pp. 545-6.
10. Y. Horie and G. E. Duvall, "Shock Waves and the Kinetics of Solid-Solid Transitions", Proceedings of the U.S. Army Symposium on Solid Mechanics, Watertown, Mass., AMMRC MS 68-09, September 1968.

LIST OF SYMBOLS

- t time, μs (subscripts 0, 1, 2, 3, and 4 refer to times in Figure 2).
- u particle velocity, m/s (subscripts e, p₁, and p₂ refer to the elastic, P₁, and P₂ waves, respectively).
- u_0 impact velocity, m/s .
- u_f free-surface velocity, m/s (subscripts 1, 2, and 4 refer to free-surfaces velocities in Figure 2).
- U wave velocity with respect to material ahead of the wave, m/s (subscripts e, p₁, and p₂ refer to the elastic, P₁, and P₂ waves, respectively).
- U^* wave velocity in laboratory coordinates, m/s .
- V specific volume, cm^3/g .
- X distance, mm (subscripts 0, 1, 2, 3, and 4 refer to distances in Figure 3).
- ρ density, kg/m^3 (subscripts 0, e, p₁, and p₂ return to unstressed material, the elastic, the P₁ wave, and the P₂ wave, respectively).
- σ stress, GPa (subscripts e, p₁, and p₂ refer to the elastic, P₁ and P₂ waves, respectively).

Subscript "i" refers in a general way to an initial condition.

DISTRIBUTION LIST

<u>No. of Copies</u>	<u>Organization</u>	<u>No. of Copies</u>	<u>Organization</u>
12	Commander Defense Documentation Center ATTN: DDC-DDA Cameron Station Alexandria, VA 22314	2	Commander US Army Missile Research and Development Command ATTN: DRDMI-R DRDMI-YDL Redstone Arsenal, AL 35809
1	Director Defense Advanced Research Projects Agency ATTN: Tech Info 1400 Wilson Boulevard Arlington, VA 22209	1	Commander US Army Tank Automotive Rsch and Development Command ATTN: DRDTA-UL Warren, MI 48090
1	Commander US Army Materiel Development and Readiness Command ATTN: DRCDMD-ST, N. Klein 5001 Eisenhower Avenue Alexandria, VA 22333	3	Commander US Army Mobility Equipment Research & Development Cmd ATTN: Tech Docu Cen, Bldg 315 DRSME-RZT STSFB-MW, Dr. J. Bond Fort Belvoir, VA 22060
1	Commander US Army Aviation Research and Development Command ATTN: DRSAV-E P. O. Box 209 St. Louis, MO 63166	2	Commander US Army Armament Research and Development Command ATTN: DRDAR-TSS (2 cys) Dover, NJ 07801
1	Director US Army Air Mobility Research and Development Laboratory Ames Research Center Moffett Field, CA 94035	1	Commander US Army Armament Materiel Readiness Command ATTN: DRSAR-LEP-L, Tech Lib Rock Island, IL 61299
1	Commander US Army Electronics Research and Development Command Technical Support Activity ATTN: DELSD-L Fort Monmouth, NJ 07703	1	Commander US Army Watervliet Arsenal ATTN: Dr. F. Schneider Watervliet, NY 12189
1	Commander US Army Communications Rsch and Development Command ATTN: DRDCO-PPA-SA Fort Monmouth, NJ 07703	1	Commander US Army Harry Diamond Labs ATTN: DRXDO-TI 2800 Powder Mill Road Adelphi, MD 20783

DISTRIBUTION LIST

<u>No. of Copies</u>	<u>Organization</u>	<u>No. of Copies</u>	<u>Organization</u>
5	Commander US Army Materials and Mechanics Research Center ATTN: DRXMR-ATL DRXMR-H, Mr. J. Dignam DRXMR-H, Dr. D. Dandekar DRXMR-T, Dr. J. Mescall DRXMR-H, Dr. S.C. Chou Watertown, MA 02172	1	Commander Naval Research Laboratory ATTN: Code 2020, Tech Lib Washington, DC 20375
1	Director US Army TRADOC Systems Analysis Activity ATTN: ATAA-SL, Tech Lib White Sands Missile Range NM 88002	1	AFWL (Tech Lib) Kirtland AFB, NM 87117
1	Deputy Assistant Secretary of the Army (R&D) Department of the Army Washington, DC 20310	1	Director Lawrence Livermore Laboratory ATTN: Dr. M. van Thiel, L-64 P. O. Box 808 Livermore, CA 94550
1	Commander US Army Research Office P. O. Box 12211 Research Triangle Park NC 27709	3	Sandia Laboratories ATTN: Tech Lib Dr. W. Herrmann Dr. L. D. Bertholf Albuquerque, NM 87115
1	Commander US Military Academy ATTN: Library West Point, NY 10996	1	Drexel Institute of Technology Wave Propagation Research Center ATTN: Prof. P. C. Chou 32nd and Chestnut Streets Philadelphia, PA 19104
3	Commander Naval Surface Weapons Center ATTN: Mr. W. H. Holt Mr. W. Mock, Jr. DX-21, Lib Dahlgren, VA 22448	3	Stanford Research Institute Poulter Laboratories ATTN: Dr. G. R. Abrahamson Dr. D. Curran Dr. L. Seaman 333 Ravenswood Avenue Menlo Park, CA 94025
2	Commander Naval Surface Weapons Center ATTN: Dr. J. W. Forbes Tech Lib Silver Spring, MD 20910	2	University of California Los Alamos Scientific Lab ATTN: Tech Lib GMX-6, Dr. J.W. Taylor P. O. Box 1663 Los Alamos, NM 87545
		1	Washington State University Department of Physics ATTN: Prof. G. E. Duvall Pullman, WA 99163

DISTRIBUTION LIST

Aberdeen Proving Ground

Dir, USAMSA
ATTN: Dr. J. Sperrazza
DRXSY-MP, H. Cohen
Cdr, USATECOM
ATTN: DRSTE-SG-H
Dir, Wpns Sys Concepts Team,
Bldg. E3516, EA
ATTN: DRDAR-ACW